

Development of a system to measure bed forms and vertical velocity profiles in a river channel

H. Koseki, A. Yorozuya, S. Kudo & Y. Iwami

International Centre for Water Hazard and Risk Management, Public Work Research Institute, Tsukuba, Ibaraki Japan

T. Kitsuda

Hydro Systems Development, Inc., Osaka, Japan

ABSTRACT: A new observation system using acoustic Doppler current profiler (aDcp) and multibeam echo sounders (MBES) are proposed to discuss flow resistance in relation to water flow, sediment transport and bed forms. The system was tested for its validity based on data of bed forms and velocity profiles, which were measured in a quasi-actual scale experiment flume with a movable bed. The measured data are verified by estimation of friction velocity considering change of velocity profiles on sand waves. The estimation found that 1)an appropriate bedload discharge equation by comparing data measured by MBES and 2)a part of relation between dimensionless shear stress and bed forms are verified by several empirical formulas proposed by Kishi & Kuroki (1973) and Yalin (1978).

1 INTRODUCTION

Flow resistance has been studied based on experimental and theoretical results. Engelund (1967) found that resistance generated by bed forms has two components: skin friction and form drag. Kishi & Kuroki (1973) modified the Engelund's relations using R/d (R = hydraulic radius, d = grain size). Yalin (1979) proposed the relation between wave steepness and bed shear stress based on experimental results. Egashira et al. (1997) derived an expression of flow resistance based on an energy dispersion function in an open channel with bedload theoretically. The above studies have been verified in experimental studies since there are no observation systems to measure water flow, sediment transport and bed forms simultaneously.

On the other hand, Yorozuya et al. (2010) developed a methodology to estimate bedload rate with acoustic Doppler current profiler (aDcp). Recently, the development of acoustic techniques has enabled swath measurement to observe the undulation of planar bathymetry with multibeam echo sounders (MBES).

To elucidate the relationship among water flow, sediment transport and bed forms in actual rivers during flooding, the authors propose an observation system with aDcp, MBES and a tethered boat for the simultaneous measurement of water flow, sediment transport and bed forms.

For the elucidation and the evaluation of the system, three topics are studied, 1) estimation of friction velocity, 2) evaluation of bedload rate equations, 3) relations between dimensionless shear stress and sand waves.

2 OBSERVATION SYSTEM

Figure 1 shows the present observation system composed of aDcp (River Pro ADCP manufactured by

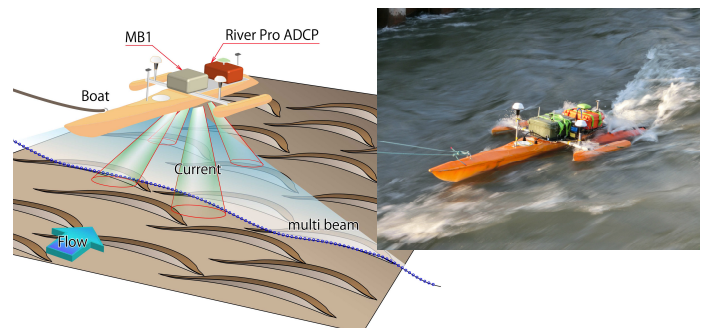


Figure 1. Observation system

Teledyne RD Instruments), MBES (MB1 manufactured by Teledyne Odom Hydrographic) and a tethered boat. The tethered boat is trimaran, main hull is about 3.0m long, side hull is 1.0m long, total weight is 33.0 kg.

MBES is installed in front of aDcp to prevent from missing data caused by bubbles generated by aDcp and boat's bottom. GPS compass is equipped with each device.

2.1 aDcp

Generally, aDcp has 4 slant beams with 20 or 30 degree and 1200 or 600kHz. It measures water velocity profiles, water depth and bedload velocity v_b . Additionally, River Pro ADCP which is used for the present study, has the fifth beam to measure water depth and vertical velocities with 600kHz.

2.2 MBES

MBES is doppler sonar system using many beams to measure bottom shape. MB1 has up to 512 beams with a frequency from 170 to 220kHz and a swath of up to 120 degrees. In the present study, it is installed at the right angles to the direction of the tethered boat. In order to measure planar bathymetry, the tethered boat takes a longitudinal round trip in the center of the channel.

3 ESTIMATION OF FRICTION VELOCITY

3.1 Methodology to estimate friction velocity

Generally, dimensionless shear stress is estimated using measured turbulent velocities or friction velocity. The former is, for example, hot-film sensors (HFS), laser-Doppler anemometer (LDA) (Nezu 1993) and aDcp (Gerbi 2008). HFS is difficult to measure due to suspended load dust and bubbles. LDA have never been conducted in rivers during flood with movable bed. aDcp have been used to measure water depth and velocity during flood, however, it is difficult to measure accurate turbulent velocities. On the other hand, the latter is practical method using observation data in actual river as below.

First method is to use energy gradient and water depth as equation (1).

$$u_* - \text{water slope} = \sqrt{ghI} \quad (1)$$

where g = acceleration of gravity; h = water depth; I = energy gradient.

Second method is based on velocity profiles measured by aDcp and uses equation (2), called u_* -log law.

$$\frac{u(z)}{u_*} = \frac{1}{\kappa} \ln \frac{z}{h} + \frac{u(h)}{u_*} \quad (2)$$

where z = distance from bed, h = water depth, $u(z)$ = water flow velocity at z , a = constant, b = constant, u_* = friction velocity, $\kappa = 0.4$.

Finally, third method uses the equation (2) in the region from bottom to local maximum to consider that the velocity profiles change due to sand waves, called u_* -author proposed by Yorozuya et al (2010).

3.2 Observation condition

Measurements were conducted by using the proposed system in a quasi-actual scale experiment flume, which is 1300 m long, 30 m wide and 1/500 in bed slope. The bed was smoothed flat initially with sand of a medium grain size of 1.5 cm. Figure 2 shows observation area, focusing on the area that is 25 m long and 8 m wide at the channel bottom. Seven water surface gauges were set in the right side of the channel bottom. The system was performed 2 to 3-minute intervals from P460 to P485. Figure 3 shows cross-section, a vertical pile sheet stands along the left bank, and concrete cover with a gradient of 45 degrees is applied to the right bank.

3.3 Observation result

3.3.1 Water flow velocity profiles

Figure 4 shows velocity profiles measured at crest and trough. Left figure shows the value measured at

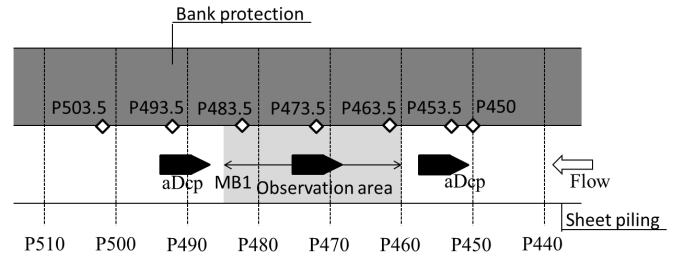


Figure 2. Location of measurement instruments for sand wave observation

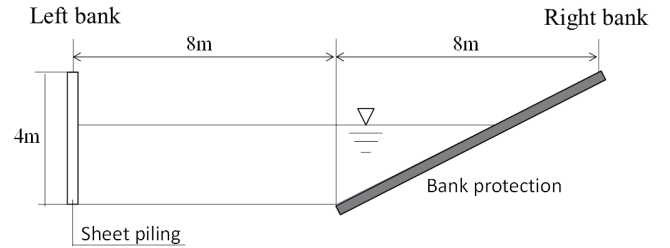


Figure 3. Cross section shape

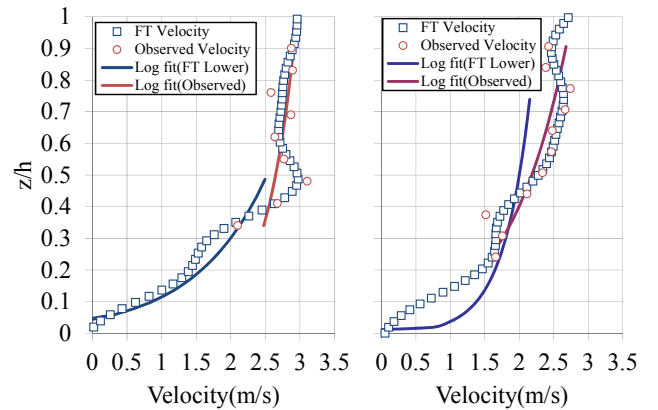


Figure 4. Water flow velocity vertical profiles (Left shows at crest, right shows at trough.)

Table 1. Friction velocity on sand waves

Parameters (unit)	Crest	Trough
u_* -authors (m/s)	0.43	0.18
u_* -log-law (m/s)	0.16	0.37
Bedload velocity(m/s)	0.55	0.15

crest, right figure shows value at trough. In each figure, red circles show measured value, red line shows approximation line of the logarithm function by measured value. Blue squares show value calculated by Fourier transformation (FT) using the measured value, blue line shows approximation line of the logarithm function by the calculated value in the region of bottom. u_* -log law is estimated by red line, u_* -author is estimated by blue line. Table 1 shows bedload velocity v_b and local friction velocity estimated by equation (2). v_b is averaged velocity of sediment transport directly measured by aDcp. Friction velocity is estimated shear stress by velocity profiles. Therefore, the friction velocity is validated by comparing with v_b . At trough, u_* -author is almost same value as v_b , and u_* -log law is twice bigger than v_b . On the other hand, at crest, u_* -author is twice bigger than v_b , and u_* -log law is a half of v_b .

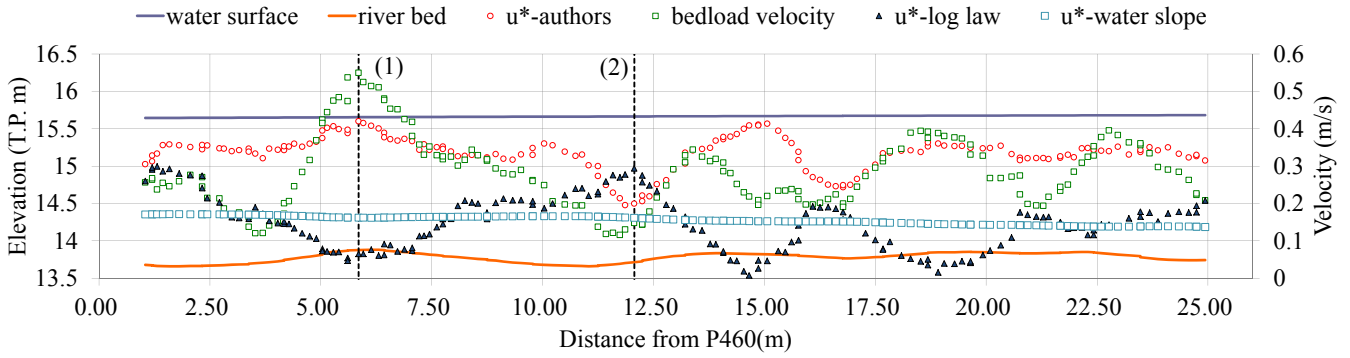


Figure 5. Change of water surface, bed elevation, bedload velocity and friction velocity (15:59-16:01)

3.3.2 Friction velocity change on sand waves

Figure 5 shows u^* -water slope, u^* -log law, u^* -author, water surface, bed elevation and v_b measured by ADCP from P460 to P485. Blue line shows water surface, brown one is bed elevation. Red circle shows u^* -author. Black triangle shows u^* -log-law. Green circle shows v_b .

Figure 4 shows velocity profiles measure at (1)crest, (2)trough in Figure 5. At crest u^* -author is bigger than u^* -log-law, at trough vice versa. v_b is in phase with u^* -author. On the other hand, v_b is in opposite phase with u^* -log law. Blue squares shows u^* -water slope estimated by using water surface gauges, P463.5, P473.5 and P483.5. u^* -water slope and v_b have no relation and underestimation than u^* -author and u^* -log law.

3.3.3 Time averaged value

Table 2 shows time averaged values measured by ADCP during the observation. u^* -author is two times bigger than u^* -log-law and u^* -water slope. Additionally, friction velocity is 0.20 using equation (1) when averaged bed slope is 1/500 and depth is 2.0m and friction velocity is 1.4 when local water slope 1/10 by image analysis. These results indicate that water surface information such as velocity is necessary to estimate appropriate friction velocity in addition to water slope.

4 ESTIMATION OF BED LAOD DISCHARGE

u^* -author is evaluated relatively in the previous topic. In this topic, absolute evaluation is conducted. To estimate bedload discharge, following measurements are conducted, measuring bed elevation change by MB1, measuring velocity profiles by aDcp.

4.1 Observation condition

Measurements were conducted in the experiment flume. Figure 6 shows observation area, focusing on the area that is 25 m long and 8 m wide at the channel bottom. Sand pit was made from P465 to P490 to

Table 2. Time averaged value measured by ADCP

Parameters (unit)	Values
u^* -authors (m/s)	0.33
u^* -log-law (m/s)	0.15
u^* -water slope(m/s)	0.16
Dimensionless shear stress(u^* -author)	0.50
Bedload velocity(m/s)	0.28
Froude number	0.49

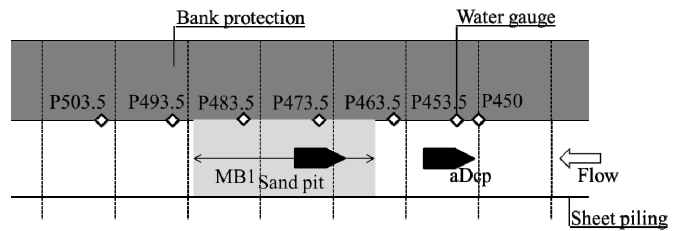


Figure 6. Channel shape and location of observation instruments

measure deposited bedload by MB1. The measurement was performed at 2 to 3-minute intervals during the observation. ADCP (Workhorse 1200kHz) measurement was conducted at P455, upstream of the sand pit.

The gate-controlled flow discharge increased at rates from 0 m^3/s to 50 m^3/s in 80 minutes, kept a constant discharge of 50 m^3/s for 110 minutes, and decreased from 50 m^3/s to 0 m^3/s in 30 minutes. Sediment feeding was not conducted.

4.2 Bed elevation change in sand pit

Figure 7 shows bed elevation in sand pit measured by MB1, left figure elevation is measured at 8:31, right figure is measured at 8:45. Flow direction is from left to right. At 8:45, elevation is higher than 8:31 in upstream of sand pit.

Figure 8 shows change of longitudinal elevation in sand pit in time series. Longitudinal axis is elevation and cross axis is distance from P450. The elevation data are picked up from Survey Line under ADCP at P455. Elevation is increasing from 16.5m to 21m. On the other hand, from 21m to 22m, elevation change is not occurred. Therefore, elevation change is determined by only input bedload discharge because output is zero.

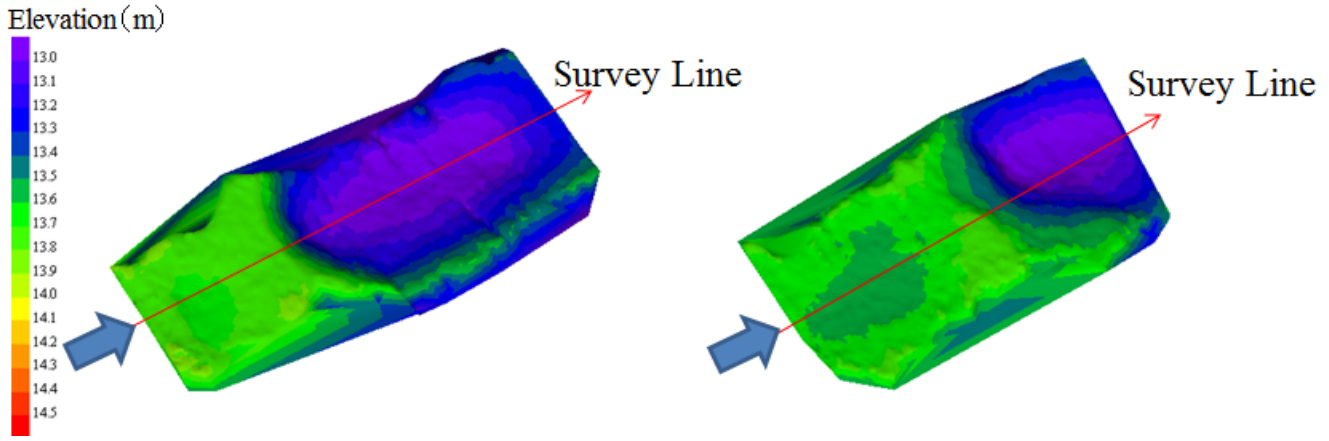


Figure 7. Bed elevation change measured by MB1 (Left elevation is measured at 8:31, Right elevation is measured at 8:45)

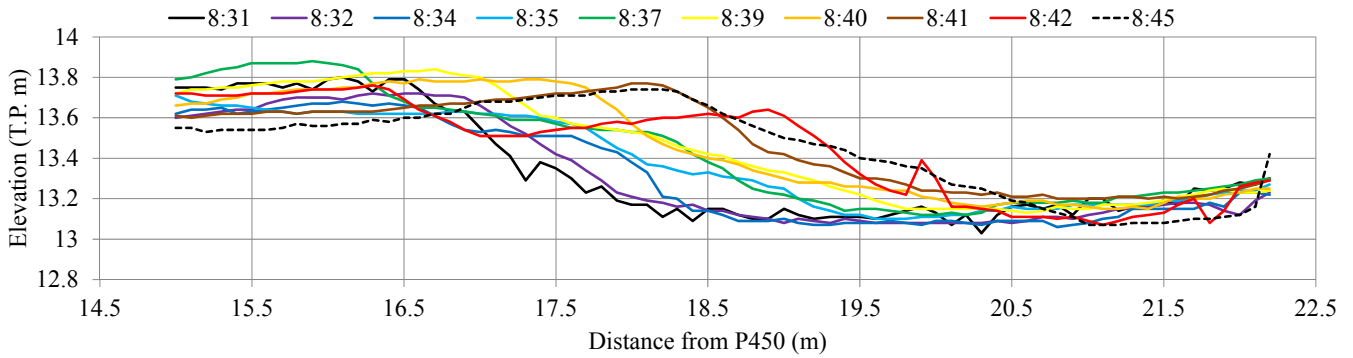


Figure 8. Bed elevation change on ADCP survey line in sand pit measured by MB1

4.3 Bedload discharge formula

Some bedload discharge equations are proposed using friction velocity. In the present study, three equations based on Bagnold equation are used as follows.

4.3.1 Egashira equation (1990, 1997)

Egashira equation has three components, sediment transport velocity u_s , bedload thickness h_s and sediment concentration c . The parameters are determined by theory.

$$q_b = \int_0^{h_s} c \cdot u \cdot dz \cong u_s \cdot h_s \cdot c_s \quad (3)$$

$$\frac{h_s}{d} = \frac{1}{c_s \cos \theta \left\{ \tan \varphi_s / (1 + \alpha) - \tan \theta \right\}} \tau_* \quad (4)$$

$$\frac{u_s}{u_*} = \frac{4}{15} \frac{K_1 K_2}{\sqrt{f_d + f_f}} \tau_* \quad (5)$$

$$K_1 = \frac{1}{\cos \theta \left\{ \tan \varphi_s / (1 + \alpha) - \tan \theta \right\}} \quad (6)$$

$$K_2 = \frac{1}{c_s} \left[1 - \frac{h_s}{h_t} \right]^{1/2} \quad (7)$$

$$f_d = k_d (1 - e^2) (\sigma / \rho) c_s^{1/3} \quad (8)$$

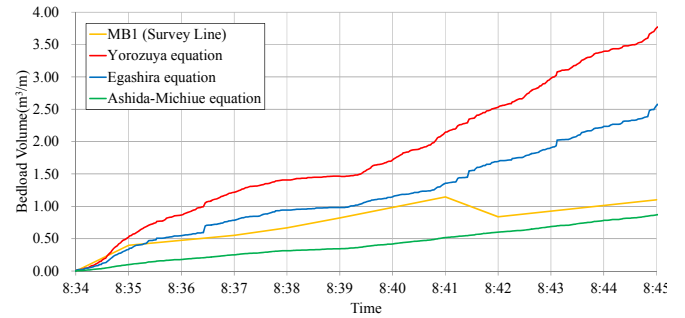


Figure 9. Bedload discharge change

$$f_f = k_f (1 - c_s)^{5/3} c_s^{-2/3} \quad (9)$$

where q_b = bedload discharge; u_s = averaged sediment transport velocity by bedload thickness h_s ; $c_s = c^*/2$ averaged sediment concentration by bedload thickness h_s ; $c^* = 0.6$ sediment concentration in non-flowing layer; d = sediment particle size; φ_s = interparticle friction angle; θ = inclination; $k_d = 0.0828$; $k_f = 0.16$; $e = 0.85$ coefficient of restitution; h_t = water depth; σ = mass density of sediment particles; ρ = mass density of water; τ_* = dimensionless shear stress. $\alpha = 0.25$ dynamic pressure/static pressure.

4.3.2 Yorozuya equation (2010)

Yorozuya equation uses v_b instead of u_s as below.

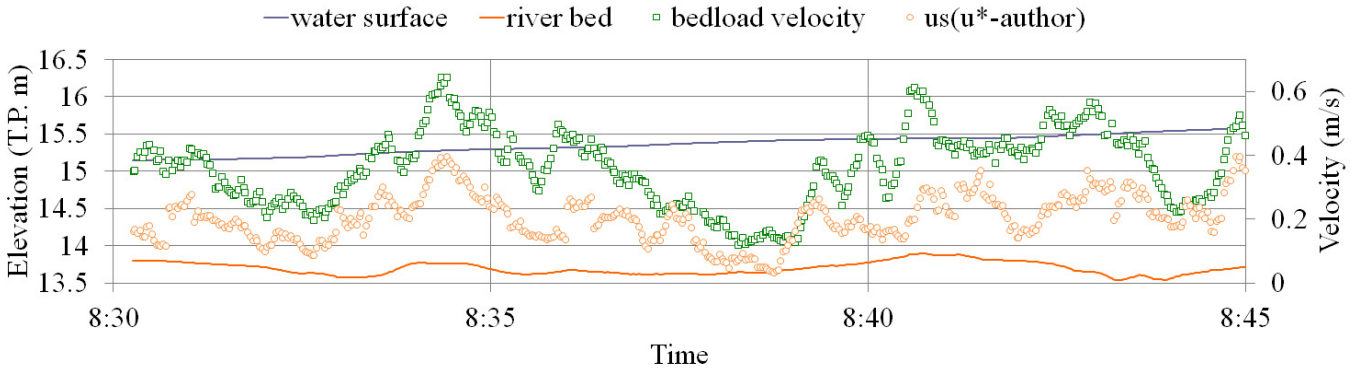


Figure 10. Timely change of velocity of sediment material and bedload velocity

$$q_b = v_b \cdot h_s \cdot c_s \quad (10)$$

where v_b = bedload velocity measured by aDCP.

4.3.3 Ashida-Michiue equation (1972)

Ashida-Michiue equation is most popular in Japan. Coefficient 17 is determined based on experimental result.

$$q_{b*} = 17 \tau_{*e}^{3/2} \left(1 - \frac{\tau_{*c}}{\tau_*}\right) \left(1 - \frac{u_{*c}}{u_*}\right) \quad (11)$$

$$q_{b*} = q_b / \sqrt{(\sigma / \rho - 1)gd^3} \quad (12)$$

$$\tau_{*e} = u_{*e}^2 / (\sigma / \rho - 1)gd \quad (13)$$

$$\frac{v}{u_{*e}} = 6.0 + 2.5 \ln \frac{h}{d(1 + 2\tau_*)} \quad (14)$$

where q_{b*} = dimensionless bedload discharge, τ_{*e} = dimensionless effective shear stress, τ_{*c} = dimensionless critical shear stress, u_{*e} = effective friction velocity, u_{*c} = critical friction velocity, h = water depth.

4.4 Observation result

4.4.1 Change of Bedload discharge

Figure 9 shows change of bedload volume. Yellow line shows MB1 result, red line shows Yorozuya equation's result, blue line shows Egashira equation's one and green line shows Ashida-Michiue equation's one. Egashira equation is in phase with MB1 result until 8:41. Yorozuya's result is about twice than MB1. Ashida-Michiue's result is a half of MB1. These results are calculated by using u^* -author. After 8:41, MB1 result is decreasing. It is possible to pass the sand waves.

Considering the relation of three kinds of friction velocity as shown in Figure 5, bedload discharge will be underestimated by using u^* -log law and u^* -water slope. Comparing equation (3) and (11), the former is function of friction velocity to the fifth power, the latter is function of friction velocity to the third power. Consequently, difference of three friction velocities greatly and absolutely affects bedload discharge.

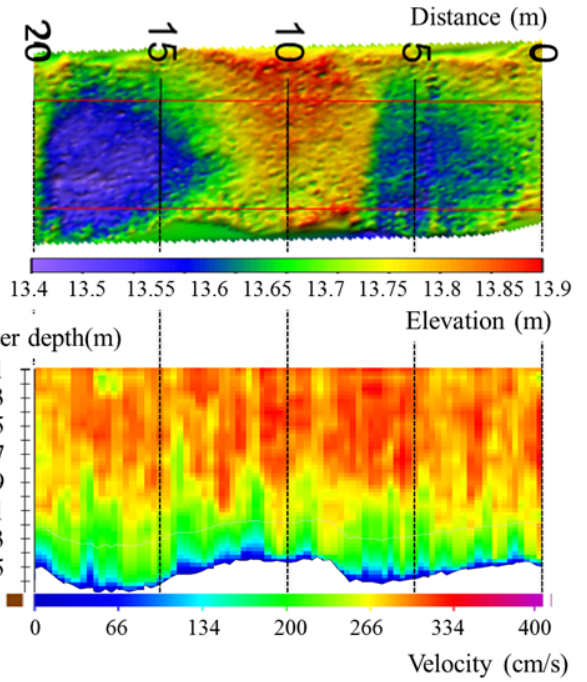


Figure 11. Bed elevation and velocity profiles (Top figure is result by MB1, bottom figure is result by ADCP)

As results of bedload observation, it is important to select not only bedload discharge equation but also estimation of friction velocity.

4.4.2 Relation between v_b and u_s

Figure 10 shows v_b and u_s in time series. They are in the same phase, hence, if u_s and v_b have a significant relation, friction velocity is estimated by equation (5). Moreover, bedload discharge is estimated by equation (3) and (4). In other words, automatic observation system for measuring bedload discharge will be applicable by using continuous observation device such as H-ADCP. Development of the relation will be conducted in the future.

5 RELATION BETWEEN FRICTION SHEAR STRESS AND SAND WAVES

Above topic shows importance of considering sand waves to estimate friction velocity. This chapter shows relation between shear stress and sand waves are validated using previous study. Observation condition is the same as Figure 3.

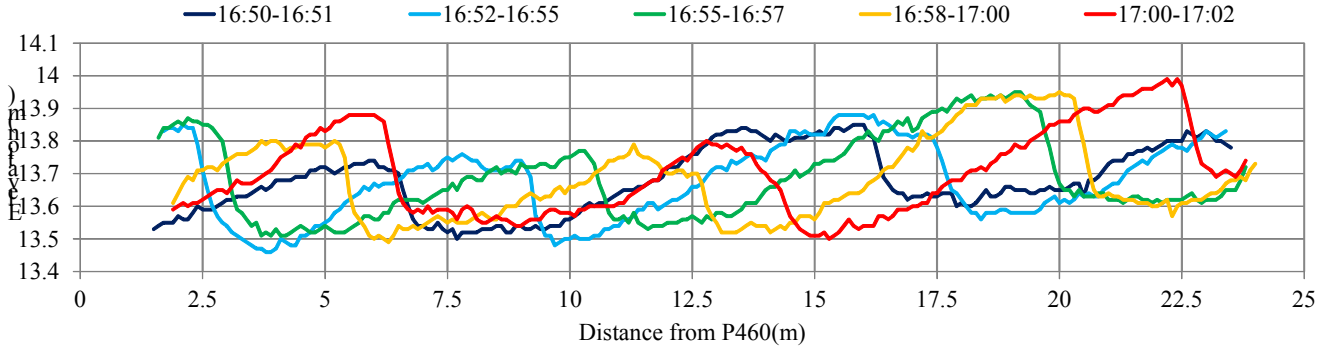


Figure 12. Bed elevation change in sand wave observation (16:50-17:02)

5.1 Observation result

5.1.1 Results of MB1 and ADCP

Figure 11 shows results measured by MB1 and ADCP simultaneously at 16:50-16:51. Flow direction is from left to right. Top figure shows result of MB1. The cross-sectional bed forms are skew. The center and right sides of the channel have almost the same wave heights and lengths while the wave height is smaller on the left side than on the other sides. The skewness is generated by the pile sheet along the left bank. Bottom figure shows velocity magnitude and water depth measured by aDcp. The water depth is in phase with bed elevation measured by MB1. Velocity profiles change according sand waves. The velocity is 2.5 m/s near bed at crest. On the other hand, at trough, the velocity is 2.0 m/s near bed.

5.1.2 Sand waves change in time series

Figure 12 shows longitudinal bed elevation measured by MB1 in time series. 5 measurements are shown. Flow direction is from left to right. During the measurement, flow discharge is constant $50 \text{ m}^3/\text{s}$. At 16:50-16:51, sand waves have two crests at 5m and 15m. The height of these crests are increasing and moving to flow direction.

5.2 Relation between dimensionless shear stress and sand waves

Yalin proposed the relation between dimensionless shear stress τ_* and wave steepness H/L (H = Wave height, L = Wavelength). Kishi & Kuroki proposed the relation between τ_* and form drag. Generally, τ_* is estimated by u_* -water slope (τ_* -water slope). τ_* -author is estimated by u_* -author. These τ_* are verified by each relation in one wavelength.

Figure 13 shows the relation proposed by Yalin (1978). Blue circle shows τ_* -water slope, red one shows τ_* -author. Where, $\tau_{*c}=0.05$, averaged $h/d=160$, $d_{50}=0.015\text{m}$. Black line is applicable to $100 \leq h/d \leq 1.04 \cdot 10^5$, broken line is applicable to $65 \leq h/d \leq 75$. Measured wave steepness is from 0.02 to 0.04. The steepness value is same in each shear stress. In τ_* -water slope/ τ_{*c} , measured wave steep-

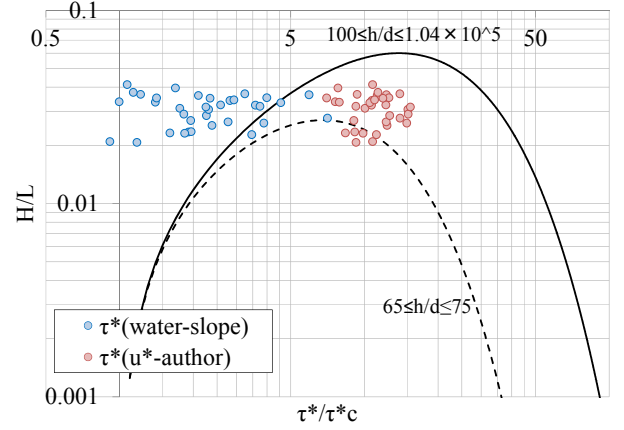


Figure 13. Relation between τ_* / τ_{*c} and H/L proposed by Yalin(1978)

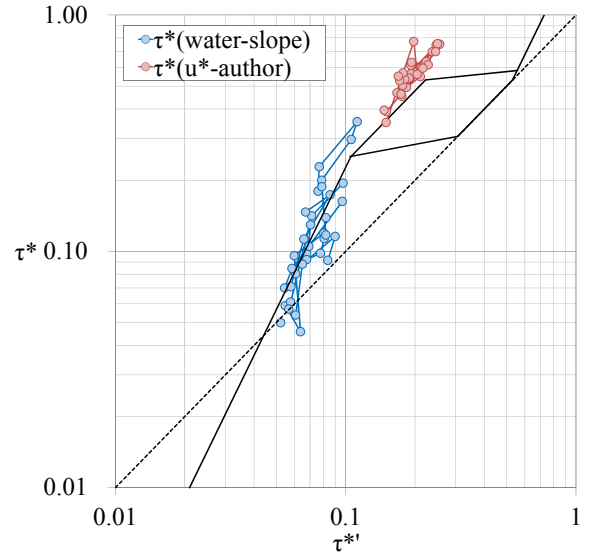


Figure 14. $\tau_* - \tau_*'$ relation proposed by Kishi & Kuroki (1973)

ness don't change by increasing τ_* -water slope/ τ_{*c} , despite the steepness increases in Yalin's relation. On the other hand, in τ_* -author/ τ_{*c} , measured data are plotted between black line and broken line, in the range of that sand waves are most developed.

To plot measured data in the relation propose by Kishi & Kuroki (1973), these equations are used.

$$u = \sqrt{gR'I} \{6.0 + 5.75 \log_{10}(R'/k_s)\} \quad (15)$$

$$\tau_* = \frac{RI}{(\sigma/\rho - 1)d} \quad (16)$$

$$\tau_* = \frac{u_*^2}{(\sigma / \rho - 1)gd} \quad (17)$$

$$\tau_*' = \frac{R'I}{(\sigma / \rho - 1)d} \quad (18)$$

where u = depth averaged velocity, I = water slope, R = hydraulic radius, R' = hydraulic radius due to skin friction, k_s = grain roughness.

When τ_* -water slope is used,

1) τ_* is calculated by using R , I and equation (16).

2) R' is calculated by using R , u and equation (15).

3) τ_*' is calculated by using R' and equation (18).

When τ_* -author is used,

1) τ_* is calculated by using u_* -author and equation (17).

2) I is calculated by using τ_* , R and equation (16).

3) R' is calculated by using I , u and equation (15).

4) τ_*' is calculated by using R' and equation (18).

Figure 14 shows the relation and measured results. Results of τ_* -water slope are plotted in the region of developed from flat to Dune I which is maximum of form drag. On the other hand, results of τ_* -author are plotted in Dune II and extension of Dune II. However, τ_*' does not increase to Transition II. It means that, in this observation, bed forms did not transit from Dune II to Transition II.

As these results, τ_* -water slope has difference in the relation between shear stress and development of sand waves. On the other hand, in case of τ_* -author, these relations are consist in the development.

6 CONCLUSIONS AND FUTURE STUDY

6.1 Conclusion

The present study proposes an observation system using aDcp, MBES and a tethered boat to measure velocity profiles and bed forms at the same time. The measured data were compared with the results obtained from previous studies regarding the relationship between water flow and bed forms. The comparison found that the following results and suggested that the system is applicable to the measurement of the channel flow and behavior of an erodible bed.

- 1) It is important to estimate friction velocity considering change of velocity profiles on sand waves. Yorozuya's estimation is validated absolutely by comparing bedload discharge.
- 2) Egashira equation agrees with directly measurement. Yorozuya equation is two times bigger than the measurement because the equation uses bedload velocity. Ashida-Muchiue equation is a half of the measurement.
- 3) τ_* -author is validated to make relation between shear stress and bed forms. In other words, water slope has less information to estimate appropriate friction velocity.

6.2 Future study

This study suggests that measuring velocity profiles is important to estimate friction velocity. However, it is difficult to measure the profiles during flood. Therefore, it is necessary to estimate friction velocity by using water surface information e.g. slope and velocity. For the purpose, estimation method is needed using the information considering bed forms.

ACKNOWLEDGEMENTS

We would like to express our deepest gratitude to Obihiro Development and Construction Department, Hokkaido Regional Development Bureau, Civil Engineering Research Institute for Cold Region in Japan for giving measurement site and data, Dr. Shinji Egashira for giving a lot of valuable advices to the measurement result, Mr. Inoue at Suimon Kankyo Co., Ltd. in Japan for producing a boat and the subcommittee of the Japan Society of Civil Engineers on improvement of discharge measurement technology for giving a lot of valuable advices to the measurement system.

REFERENCES

- A. Yorozuya, S. Okada, K. Ejima, Y. Kanno and K. Fukami, 2010. Method for Estimating Shear Velocity and Bedload Discharge with Acoustic Doppler Current Profiler, *Annual Journal fo Hydraulic Engineering*, JSCE, Vol.54, pp.1093-1098
- Engelund, F. 1967. Closure to "Hydraulic Resistance of Alluvial Streams." *Journal of the Hydraulics Division*, ASCE, Vol.93, No. HY-4, pp.287-296.
- G. Gerbi., J. Trowbridge, J. Edson, A. Plueddemann, E. Terray, and J. Fredricks, 2008, Measurements of momentum and heat transfer across the air-sea interface. *J. Phys. Oceanogr.*, 38, 1054-1072.
- I. Nezu, A. Tominaga and H. Nakagawa, 1993, Field measurements of river turbulence and secondary currents in straight rivers, *J. Hydraulic Eng.*, ASCE, No.467, II-23, pp.49-56.
- K. Ashida, M. Michiue, 1972, Study on Hydraulic Resistance and Bed-load Transport Rate in Alluvial Streams, *Transactions of JSCE* 206: 59-69.
- M. Hino, Y. Miyanaga, 1977, Analysis of Two-dimensional Flow in a Wavy Conduit, *Transactions of JSCE* 264: 63-75.
- S. Egashira, K. Miyamoto, T. Itoh, 1997. Constitutive Equations of Debris-Flow and Their Applicability, *Proc. of 1st International Conference on Debris-flow Hazards Mitigation*, C. L. Chen (Eds.), ASCE: NewYork; pp. 340-349
- T. Kishi, M. Kuroki, 1973. Bed Forms and Resistance to Flow in Erodible-Bed Channels (I), *Bulletin of the Faculty of Engineering, Hokkaido University*, 67: 1-23
- Yalin, M.S. and Karahan, F. 1978. Steepness of sedimentary dunes, *Proc. ASCE*, Vol.105, HY4, pp.381-392